FEATURE ARTICLE

Empirical BRDF Model for Goniochromatic Materials and Soft Proofing With Reflective Inks

Alina Pranovich, *Linköping University, 581 83, Norrköping, Sweden*
Jeppe Revall Frisvad, *Technical University of Denmark, 2800, Kongens Lyngby, Denmark*
Sergiy Valyukh, Sasan Gooran, and Daniel Nyström, *Linköping University, 581 83, Norrköping, Sweden*

The commonly used analytic bidirectional reflectance distribution functions (BRDFs) do not model goniochromatism, that is, angle-dependent material color. The material color is usually defined by a diffuse reflectance spectrum or RGB vector and a specular part based on a spectral complex index of refraction. Extension of the commonly used BRDFs based on wave theory can help model goniochromatism, but this comes at the cost of significant added model complexity. We measured the goniochromatism of structural color pigments used for additive color printing and found that we can fit the observed spectral angular dependence of the bidirectional reflectance using a simple modification of the standard microfacet BRDF model. All we need to describe the goniochromatism is an empirically based spectral parameter, which we use in our model together with a specular reflectance spectrum instead of the spectral complex index of refraction. We demonstrate the ability of our model to fit the measured reflectance of red, green, and blue commercial structural color pigments. Our BRDF model enables straightforward implementation of a shader for interactive preview of 3-D objects with printed spatially and angularly varying texture.

Structural colors appear in nature and have been classified as a distinct category for several reasons. The main reason is the nature of how these colors are formed, namely via interference and diffraction of light waves on nano- to micrometer structures. These processes usually depend on wavelength and direction, which is referred to as goniochromatism, or a point in a material changing its color when observed or illuminated from different directions. The term structural colors is sometimes used interchangeably with iridescent colors due to the remarkably high saturation that is not achievable by traditional pigments and dyes.

Digital Object Identifier 10.1109/MCG.2024.3391376
Date of publication 19 April 2024; date of current version 25 October 2024.

Diffraction gratings on CDs as well as some bird feathers and butterfly wings are examples of surfaces exhibiting structural colors. Thin films of transparent materials are good sources of structural colors and are in practice applied as coatings. Individual micro particles known as grounded mica flakes can be coated with a thin film to enable controlled fine placement of differently thick films across an object surface.[1] Such fine placement is essential in printing, for example, where spatial arrangement of particles with a limited number of colors can result in patterns perceived as including a number of shades and combinations of the used primaries.[2]

Commercial coated mica particles are referred to as structural color pigments, for their combined optical properties of coatings and size and mobility. Their reflective properties allow reproduction of iridescent colors using traditional printing techniques.

In printing, one of the benefits of being able to judge the outcome of the print before the actual print

is produced. Digital visualization of real materials exhibiting structural colors is a problem that has been addressed only partially. For the ideal coatings, one may refer to the optical calculations providing the reflected spectrum and intensity for a given angle of incidence and material parameters. However, in practice, the ideal homogeneous thin film assumption is too simple. Factors such as roughness and unevenness of the substrate below the thin film, or like in case of coated mica particles, their distribution in the volume and orientation dramatically affect the observed surface color. Particularly in printing, these real world macro parameters are hard to represent theoretically, as they are produced by a combination of printing medium, paper, and an algorithm transferring a digital image into a printing recipe.

We propose an analytic bidirectional reflectance distribution function (BRDF) for straightforward rendering of goniochromatic structural colors. Using the example of commercially available structural pigments reflecting in red, green, and blue bands, we prepare samples, obtain measurements of their goniochromatic reflectance properties, and subsequently model them with a modified microfacet BRDF function. Our model uses a normal distribution function like other microfacet-based BRDF models but then replaces the other terms with a spectral/colored reflectance multiplied by an exponential function applied to a term that depends on another spectral/colored parameter and half the sum of the angles of incidence and observation. This model is easily implemented as a shader for real-time preview of prints.

RELATED WORK

Surfaces with geometric features in a size range similar to the wavelength of the light exhibit diffraction and interference effects. These can lead to a goniochromatic BRDF, meaning that the part of the function that depends on the directions toward the light and the observer also depends on the wavelength.[3,4,5] The BRDF model becomes particularly complicated for the case of pearlescent materials, which combine thin films and particle scattering in the wavelength size range.[6,7,8] As an alternative to the complex physically based models, we propose capturing the goniochromatism observed in physical materials using a practical empirically based modification of a commonly used microfacet BRDF.

The microfacet BRDF approach aims to provide a realistic representation of rough surfaces. Initially, the concept involves dividing a rough surface into numerous individual pieces, each of which is assumed to be sufficiently homogeneous and larger than the wavelength of light. This sizing allows the application of ray optics when describing the behavior of individual microfacets. The BRDF of a rough surface is then expressed statistically through the distribution of microfacet surface normal relative to the macrosurface normal. The commonly used Torrance–Sparrow BRDF model[9] was introduced to graphics by Blinn[10] including the microfacet normal distribution function proposed by Trowbridge and Reitz.[11] Walter et al. [12] presented an extension of the Torrance–Sparrow BRDF to include transmittance and referred to the Trowbridge–Reitz distribution as the GGX distribution. Due to the fatter tail of the GGX distribution, it has a tendency to better fit measured reflectance and transmittance data.[11,12,13] We take our outset in the Torrance–Sparrow BRDF with the GGX distribution and modify this with a different angle-dependent term to model goniochromatism.

Some work is dedicated to rendering of diffraction effects in periodic 2-D structures[14,15] or an explicitly defined patch of microgeometry,[16] or rendering of the interference effects in plane-parallel thin films.[17] The reflectance model is then based on theory from optics. Our model is empirically based and much simpler to work with. Our aim is to model the angular reflectance properties observed in available goniochromatic samples. Specifically, we refer to samples consisting of particles coated with titanium dioxide (TiO_2). The layer thickness on the individual particles is not necessarily homogeneous and the particles can be stacked one after another. This essentially modifies the reflectance spectrum of the surface.

MATERIALS

We approach goniochromatism with an emphasis on robust, practical, and user-friendly rendering of structural color materials/pigments/inks. Our aim is to faithfully represent the reflectance properties of real target materials. To this end, we chose commercially available so called RGB pigments produced by Merck. Individual mica particles are coated by a thin layer of TiO_2. The thickness of the film influences the reflectance spectrum and is optimized for reflectance in red, green, and blue. Each primary pigment produces the appropriate color under specific combinations of incident light and viewing direction.[18,19] However, nonoptimal conditions can lead to reduced color saturation and a shift toward gray hues. Interestingly, the raw pigment powder appears white in bulk, and the true color of each pigment becomes apparent only when spread as a layer. The specific distribution of the

FIGURE 1. Patches printed with RGB primaries. Top: Screen printed with the conventional ink preparation method. Bottom: Printed with our brushing-based method. The appearance of the patches improved toward a homogeneous, strongly reflecting surface.

particles within the volume thus plays a crucial role in the final color appearance. Iridescent colors have been produced by printing with these RGB pigments[20] and their light reflection properties were considered useful in security and hologram printing.[21] These references focus on the printing technique and do not provide the tool we suggest for preview of the angle-dependent appearance of the prints to be made.

In printing, varying R, G, and B levels of a digital image need to be replaced by spatial distribution of binary placement of primaries. As a result, printing input consists of a number of logical 2-D arrays representing on what positions in the print each ink will be placed (through halftoning algorithm). Halftoning algorithms may vary depending on specific printing application. In case of printing with R, G, and B primaries like in case of commercial pigments, there will be three channels. It is important to be able to preview all binarized channels together in order to judge the color reproduction, and halftoning algorithms. In addition, light reflecting properties of thin film coated mica flakes are affected by the individual surface structure of the flakes. The same applies to a patch printed using inks based on coated mica pigments as individual particles can align with some degree of freedom, effectively varying direction of incident light within the patch.

A specific printing technique and process of mechanical application of the RGB inks can vary. Hence, surface properties of the final print are combination of all of these factors. Therefore, in our work, we start with collecting reflective properties of special effect pigments used in real printing conditions.

We aim at representing each individual material with minimal stored data and calculation effort to obtain a practical analytic BRDF model.

PREPARATION AND MEASUREMENT

We prepared samples for BRDF measurement by printing flat patches filled with each type of pigment. Due to the relatively large size of the coated

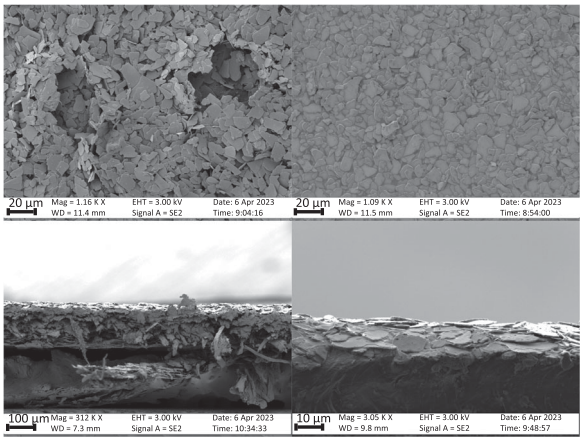

FIGURE 2. SEM images of printed areas with binder-pigment inks (left) and our method (right). Top: Top views at the same scale. Bottom: Cross-sectional views in different scales. The top view demonstrates that our method achieves a smooth and homogeneous surface, effectively assuring a 100% coverage of the printed area by the primary pigment. The scale is smaller in the cross-sectional view of our method as the particle layer is very thin (nearly no stacking of particles).

mica pigment particles (5 to 20 μm), the number of suitable printing methods is limited. We chose screen printing and initially followed the producer's guidelines for preparation of ink based on the pigment. According to those, pigment powder should be mixed with a binding medium in a concentration of 25% to produce a viscous mass that can be applied on a substrate. Produced prints showed pastel colors with low saturation (Figure 1, top). The most likely reason is that individual particles have the freedom to orient themselves in the binding medium, and internal air bubbles create significant distribution in orientation, as seen in the scanning electron microscope image in Figure 2.

To achieve the best possible color, particles need to be placed as flatly as possible. We achieved this by modifying the screen printing procedure. Specifically, we replaced the ink mixing step with brushing dry pigment powder on top of an adhesive medium. In this way, we effectively achieved a 100% concentration of pigments across a substrate area. Figure 1 demonstrates the color and general surface appearance of the patches printed with the conventional binding medium and with brushing. In agreement with the observed appearances of the patches, the electron microscope photographs in Figure 2 demonstrate a smoother particle

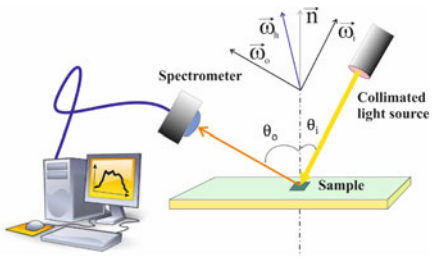

FIGURE 3. Experimental setup for in-plane BRDF measurement.

placement and alignment within a thin layer for our brushing-based method.

Our bespoke printing method is useful for measuring the intrinsic reflectance properties of the reflective inks, as this method provides the best colors we could achieve with the given pigments. We printed on black substrate, following the guidelines. To model other printing processes than our bespoke method, we let the roughness parameter of a microfacet surface normal distribution represent particle misalignments. As a consequence, the roughness parameter of our model depends on the choice of printing technique and substrate. We measure the goniochromatic properties of the coated particles and fit a model to obtain a surface roughness. We consider this roughness minimal and assume that more imperfect printing techniques are adequately modeled by increasing the roughness.

To quantify the angle-dependent color properties of the printed samples, we employ a setup consisting of a collimated light source, goniometer, and spectrometer, illustrated in Figure 3. Prior to measurements, we perform a calibration procedure using a 99% Spectralon. The spectrometer averages all incident light collected within its solid angle of observation and provides an observed spectrum. Measurements were carried out over a directly illuminated area of about 4 mm in diameter. For each measurement, ten spectra were collected and subsequently averaged. No near-field effects were captured in this relatively large area of observation. We divided the obtained reflectance values by those obtained from the white reference to obtain BRDF values.[22] Reflectance spectra were captured with this instrument for θ_i at every 10° from 20° to 70° and additionally at 65° because of low confidence for measurements at 70° (due to geometrical constraints). Obtained wide reflectance spectra were trimmed to 380 to 780 nm with 10 nm resolution (sufficient for conversion to a color space).

BRDF MODEL

Digitally, the visual properties of a material under different viewing and lighting conditions can be represented in the form of a suitable model that takes into account material properties, goniochromatic behavior, and roughness. A rigorous optical model would require knowledge of spectral complex refractive indices of TiO_2 and mica, thickness of the TiO_2 layer, parameters of other involved media, roughness of the mica flakes (or other substrate), and individual particle orientation. Our choice is to look for an empirical and practical model, rather than a rigorous physical one. We need to capture the wavelength-dependent reflectance peak as a function of the angle of incidence of the light, and the broadening of the peak around the specular direction of reflection caused by the surface roughness. To describe the latter, we turn to one of the existing approaches.

We take an outset in the Torrance–Sparrow BRDF model[9] with the Trowbridge–Reitz microfacet normal distribution function,[11] also called the GGX distribution.[12] Since this BRDF model is isotropic and symmetric around the projected deviation vector,[23] in-plane measurements of the BRDF contain enough information to fit the model. Letting λ denote wavelength while $\vec{\omega}_i$ and $\vec{\omega}_o$ are the unit vectors in the directions toward the light and the observer, respectively, the half-angle vector is

$$\vec{\omega}_h = \frac{\vec{\omega}_i + \vec{\omega}_o}{\|\vec{\omega}_i + \vec{\omega}_o\|}. \tag{1}$$

If the surface normal is $\vec{n}$, the cosine of the half angle is $\cos\theta_\mathrm{h} = \vec{\mathrm{n}} \cdot \vec{\omega}_\mathrm{h}$, the cosine of the difference angle is $\cos\theta_\mathrm{d} = \vec{\omega}_\mathrm{i} \cdot \vec{\omega}_\mathrm{h}$, and we have $\cos\theta_\mathrm{i} = \vec{\mathrm{n}} \cdot \vec{\omega}_\mathrm{i}$ and $\cos\theta_\mathrm{o} = \vec{\mathrm{n}} \cdot \vec{\omega}_\mathrm{o}$. The Torrance–Sparrow BRDF is then

$$f_r(\vec{\omega}_i, \vec{\omega}_o, \lambda) = \frac{F(\cos\theta_\mathrm{d}, \lambda)\mathrm{G}(\vec{\omega}_\mathrm{i}, \vec{\omega}_\mathrm{o})\mathrm{D}(\cos\theta_\mathrm{h})}{4\cos\theta_\mathrm{o}\cos\theta_\mathrm{i}} \tag{2}$$

where F is Fresnel reflectance, G is a geometric attenuation term, and D is a microfacet normal distribution function. The GGX distribution is[10,11,12]

$$D(\cos\theta_\mathrm{h}) = \frac{\alpha^2}{\pi((\alpha^2 - 1)\cos^2\theta_\mathrm{h} + 1)^2} \tag{3}$$

where positive α between 0 and 1 is associated with the surface roughness.

Since goniochromatism is due to multiple scattering and diffraction effects in the interaction between light and microfacets, we replace F, G, and the cosine terms in the denominator with another term. Inspecting our data, the reflectance values seem to increase

following an exponential function as the angle of incidence or observation increases. We found the following function a replacement for the mentioned terms of the standard model that better fits our measured data:

$$E(\cos\theta_\mathrm{i}, \cos\theta_\mathrm{o}, \lambda) = \rho(\lambda)\exp\left(c(\lambda)\left(1 - \cos\frac{\theta_\mathrm{i}+\theta_\mathrm{o}}{2}\right)\right). \tag{4}$$

Inserted in (2) in place of F, G, and the cosines, we arrive at the following BRDF model:

$$f_r(\vec{\omega}_i, \vec{\omega}_o, \lambda) = \frac{\alpha^2\rho(\lambda)\exp\left(c(\lambda)\left(1 - \cos\frac{\theta_\mathrm{i}+\theta_\mathrm{o}}{2}\right)\right)}{4\pi\left((\alpha^2-1)\cos^2\theta_\mathrm{h}+1\right)^2} \tag{5}$$

where ρ is a spectral reflectance and c is a spectral coefficient that represents the goniochromatism of the material. This happens since c is not just a factor of proportionality, its effect changes nonlinearly with the angles of incidence and observation. We set the surface roughness α to a constant for all wavelengths and directions.

The parameters controlling our BRDF model are thus α, ρ, and c out of which the latter two are defined by a spectrum. Our BRDF model is easily implemented in a shader. To make its use practical, where we usually have the cosines available rather than the angles, we use (since the inclination angles are in the first quadrant):

$$\cos\frac{\theta_\mathrm{i}+\theta_\mathrm{o}}{2} = \frac{1}{2}\left(\sqrt{(1+\cos\theta_\mathrm{i})(1+\cos\theta_\mathrm{o})} - \sqrt{(1-\cos\theta_\mathrm{i})(1-\cos\theta_\mathrm{o})}\right). \tag{6}$$

Given the parameters for reflective RGB pigments, we can then render the expected appearance of a print.

Since our model is spectral, we use an emission spectrum for the luminaire in a scene and convert the shading result to RGB values by means of the xyz color matching functions and conversion from XYZ to RGB as described by Cook and Torrance.[24]

FITTING PROCEDURE

Using nonlinear least squares fitting,[25] we fit our model (5) to the collected measurements in two steps. Averaging reflectance across the spectrum, we first recover the wavelength-independent roughness parameter α by fitting this averaged data to an arbitrarily scaled GGX distribution (3). We obtain one roughness value for each angle of incidence with standard deviation below 3% of the mean value. This indicates that we can safely use the average of the obtained values for α. After estimating the roughness parameter, we fit obtained reflectance values for configurations capturing perfect specular reflection specular directions. In this specific case, our BRDF (5) becomes

$$f_r(\vec{\omega}_i = \vec{\omega}_o, \lambda) = \frac{\rho(\lambda)\exp(c(\lambda)(1-\cos\theta_\mathrm{i}))}{4\pi\alpha^2} \tag{7}$$

with α fixed. In this step, the parameters ρ and c are retrieved per wavelength, resulting in the final spectral parameters for the material model.

Figure 4 (top) shows our BRDF measurements of red, green, and blue reflective inks averaged across the spectrum and the fitted functions. While we measured the BRDF for angles of incidence from 20° to 70°, geometric limitations of our setup resulted in low confidence for the data at 70°. For this reason, measurements at $\theta_i = 70°$ were not included in our fits. The result of the fits is an estimated roughness of $\alpha = 0.19$ for all three pigments. Figure 4 (bottom) plots the obtained spectral parameters ρ and c for all three primaries.

RESULTS

We implemented a shader evaluating our BRDF model (5) for wavelengths at every 10 nm from 380 to 780 nm (the visible part of the spectrum). We stored spectral parameters in a texture: ρ and c for each ink, luminaire emission, and the xyz color matching functions. Once the BRDF has been evaluated for each wavelength and each light source, the shader uses the xyz color matching functions and an XYZ to sRGB conversion to return an RGB vector. To enable inspection in a browser with interactive view control, our implementation is in WebGL and available together with a table listing the spectral parameters at https://people.compute.dtu.dk/jerf/rgbink.

For comparison, we implemented the standard Torrance–Sparrow model (2) and used the spectral complex refractive index of TiO_2 for the Fresnel equations (as the TiO_2 layer around the mica particle is first encountered by an incident light ray). However, this does not model the color of the underlying pigment, so we multiply the result of the Fresnel term by our fitted ρ. The intensity of the reflection is then a bit low, so we also tested use of the Schlick approximation[26] in which we can insert our fitted ρ. The Schlick approximation provides a more accurate overall intensity compared to our model except at grazing angles, where it becomes a bit too intense.

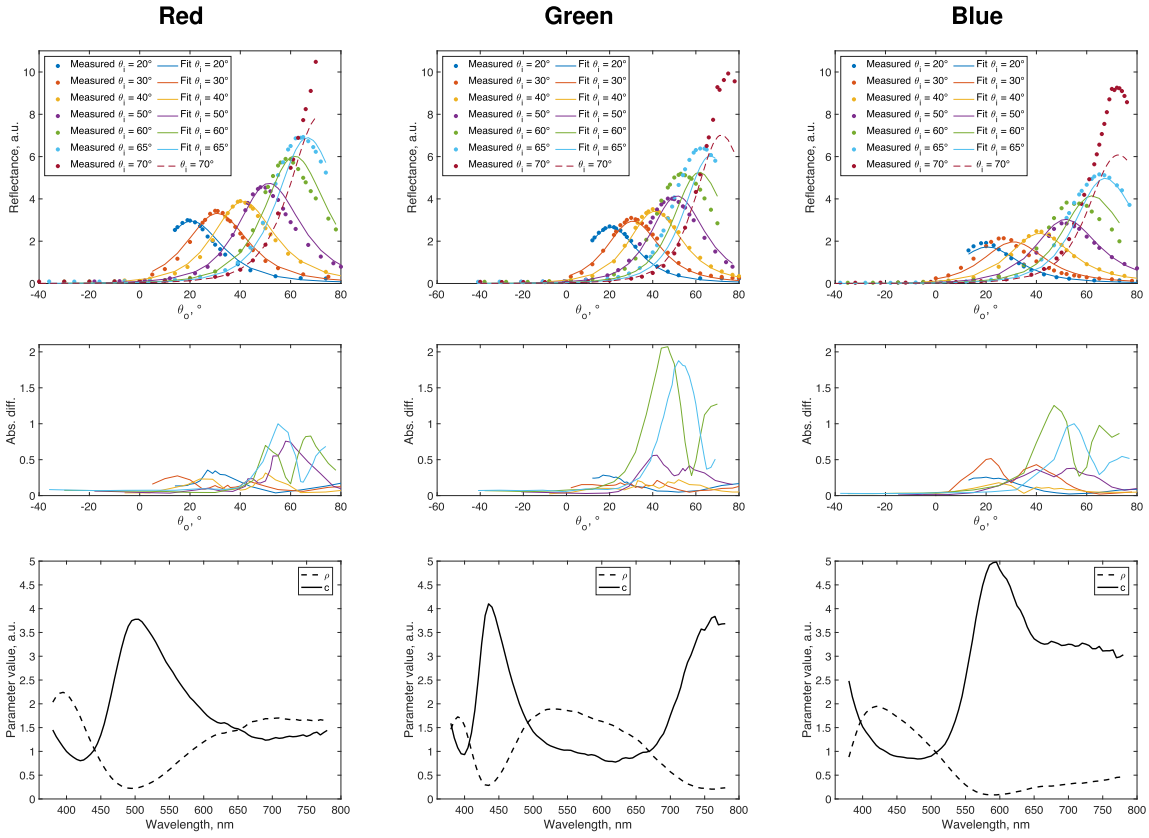

FIGURE 4. Top: Measured reflectance of the primary pigments averaged over the spectrum (dots) and model fit (curves). These plots demonstrate the exponential behavior of the reflectance. Middle: Absolute difference between measured data and fit, mostly caused by angular measurement error. Bottom: Final parameters of the primaries to be stored in the shader.

Figure 5 shows renderings of spheres each covered with red, green, or blue reflective ink for different roughness parameters. We use two directional lights to demonstrate the difference in appearance for different light-view configurations expected in goniochromatic materials. Our model clearly exhibits a different color (goniochromatism) at grazing angles of incidence/observation. This goniochromatism is not captured by the standard Torrance–Sparrow model.

PRINTING APPLICATION

Since the selected materials for this work are used in printing, we here describe the use of our model in a procedure for soft proofing (previewing) of future prints. In printing, a limited number of colors (primaries) are used to reproduce a full color digital image coded with varying R, G, and B levels. Halftoning is employed to overcome the lack of physically available hues. The idea behind halftoning is to replace digital levels in either the R, G, or B channel by spatial binarized placement of available colors. For example, 0.3 level of R in a certain pixel would correspond to a square of 3×3 pixels where only three pixels will be filled with color, the rest are left empty. A halftoning example is shown in Figure 6. For a human observer, the spatial resolution is lost when small printed dots are observed at a reasonable distance, resulting in effective mixing of tones, similar to the one achieved by tuning digital RGB levels.

Before producing a physical print, it is important to be able to preview the expected result. This is especially important for printing techniques like screen printing, where the physical print involves production of a special frame with halftone pattern burnt into it (one per channel, or 3 for an RGB image). A preview option would enable iterations and reviews of the print preparation. When printing with materials similar to the ones studied in this work, previewing the outcome under varying illumination and observation conditions is very beneficial.

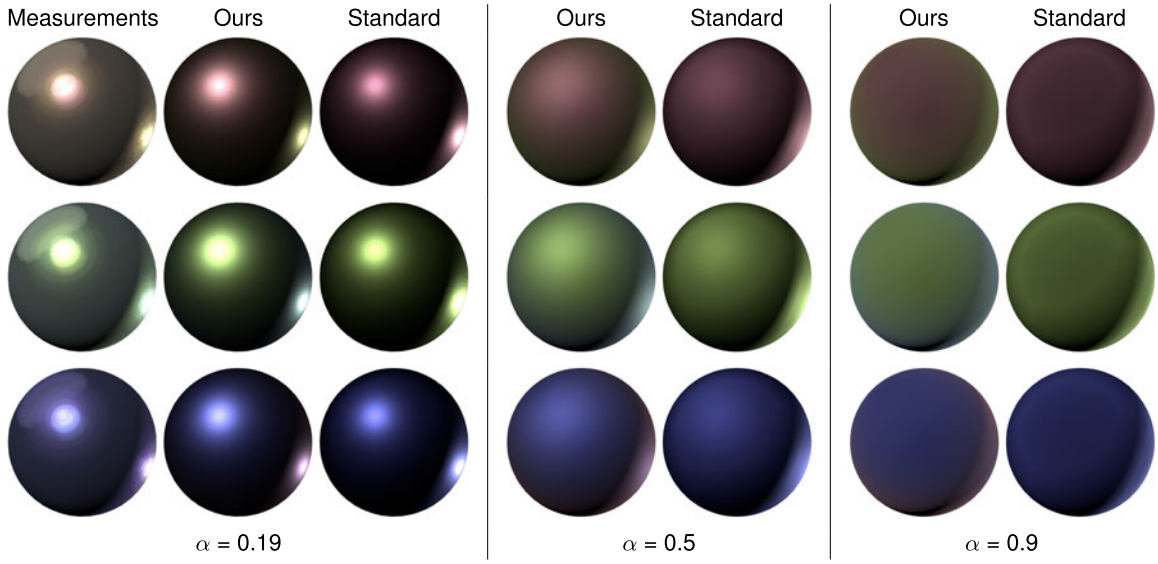

FIGURE 5. Red, green, and blue reflective inks with different roughness parameters on a sphere illuminated by two directional lights. For each material, we compare the result of our BRDF model with that of the standard Torrance–Sparrow BRDF model (Schlick approximation of Fresnel). The goniochromatism (color difference) produced by our model at grazing angles of incidence and/or observation is not captured by the standard model. We also rendered the spheres using filtered averaging of the measurements (leftmost column) based on the four nearest neighbors in projected deviation vector coordinates. A quantitative comparison of these results is in Table 1.

To combine the RGB reflective inks as in a print, we use texture mapping. We store the halftoning patterns for the three different primaries in an RGB texture (see Figure 6). Unlike classical texture, we reserve R, G, and B values to be 0 or 1, indicating the absence or presence of the corresponding pigment color. For the specific material shown in this work, a halftoning process that avoids placement of two different primaries in the same location is preferred.[2] The input texture is a three channel image (RGB) with no overlapping colors. The colors are either fully or not at all saturated. In the shader, we can then use the coefficients of the material that is present in the texture. To avoid branching, we simply retrieve the parameters of all three primary materials and dot them with the RGB halftoning texture value.

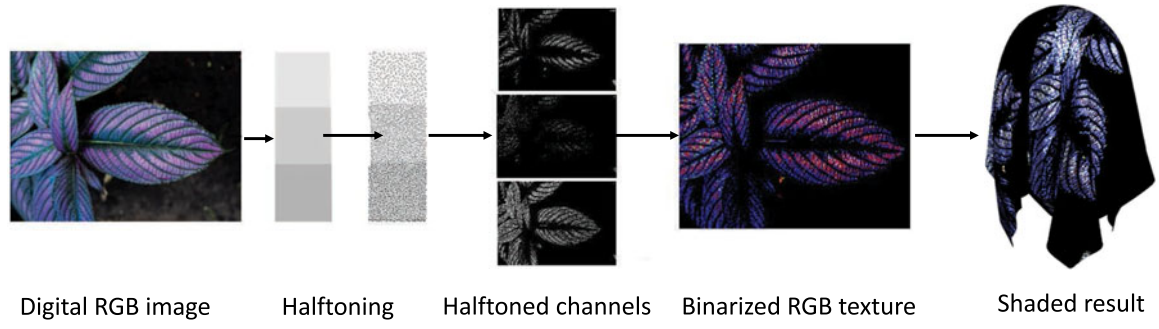

FIGURE 6. Schematic of our soft proofing (preview) process for prints with RGB reflective inks. A digital image is rasterized by repositioning fractional levels of R, G, and B primaries in a spatial distribution of 0 and 1 levels of primaries (halftoning), which is a mandatory part of every printing process. Separate channels are merged into a single RGB image. This image is used as texture mapped onto a 3-D geometry.

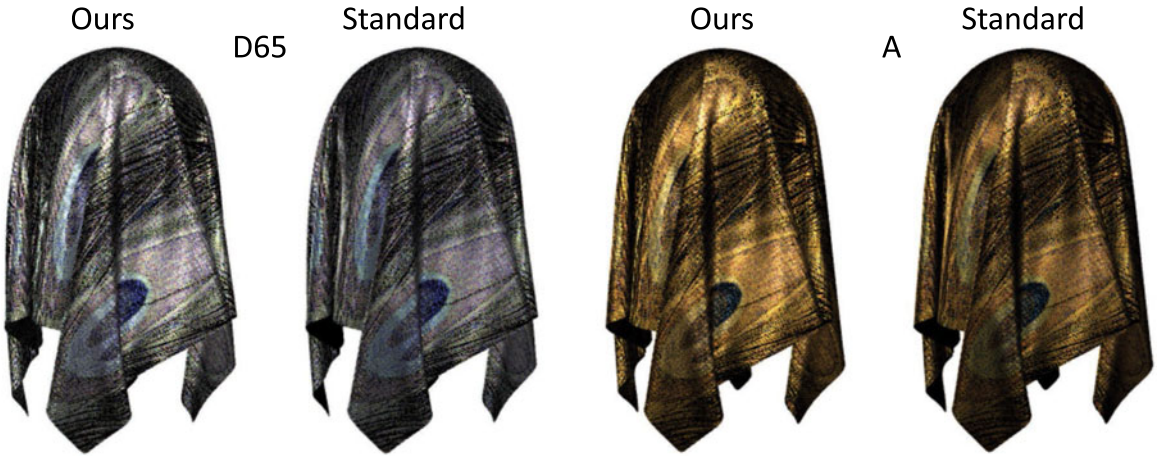

FIGURE 7. Demonstration of mapping halftoned texture onto a 3-D shape under illumination D65 (left) and A (right). We show the rendered result of our BRDF model and the standard Torrance–Sparrow BRDF model. The differences between the two models are more obvious in an interactive session with free camera control.

Figure 7 shows an example of a binarized halftoning texture applied on a 3-D model under illuminants D65 and A. Finally, we photographed a scene consisting of a curved physical print illuminated by a point-like source. We measured the emission spectrum of the source and modeled a digital scene aligned with the physical scene to enable comparison of the photo with our rendered result. The result is in Figure 8. One shortcoming of our model is that it does not include transmission of light. To mitigate this problem and improve the match between photo and rendering, we added a dim texture-independent Phong highlight with a very low shininess[27] as well as single scattering[28] to model the weak reflection from the black substrate beneath the thin layer of reflective ink. In addition, we added a dim directional light illuminating the sample from the opposite side to mimic the light transmitting through the black paper and reaching the shadowed region. Figure 9 shows what the rendering looks like without this secondary light and when using the standard model while including the secondary light.

TABLE 1. Due to the sparsity of measured configurations, the spheres rendered using measurements are not perfect as references. Even so, we report here the root-mean-squared error [(RMSE) lower is better] and the structural similarity index [(SSIM) higher is better] of our model and the standard model as compared with the renderings based on measurements. We also include rendering time for a frame of resolution 512×512 rendered using an NVIDIA RTX 4080 laptop GPU.

Model	Pigment	RMSE	SSIM	Render Time
Ours	Red	0.1182	0.7557	107 μs
	Green	0.1163	0.7159	
	Blue	0.0792	0.8034	
Standard	Red	0.1495	0.6096	116 μs
	Green	0.1444	0.5978	
	Blue	0.1020	0.7329	

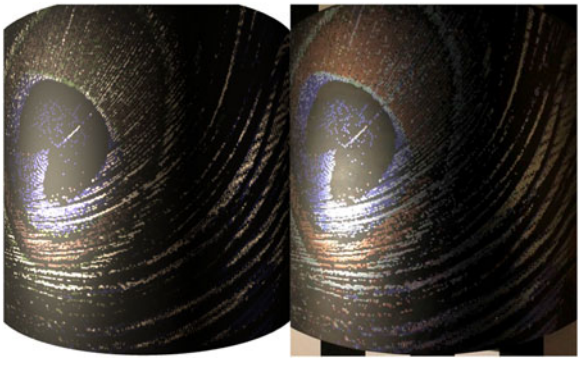

FIGURE 8. Rendering and photograph aligned and juxtaposed for qualitative comparison. Left: Preview rendered using our model. Right: Photo of a curved physical print on black paper. A dim secondary light source was added in the virtual scene to model light transmitted to the shadowed region of the article.

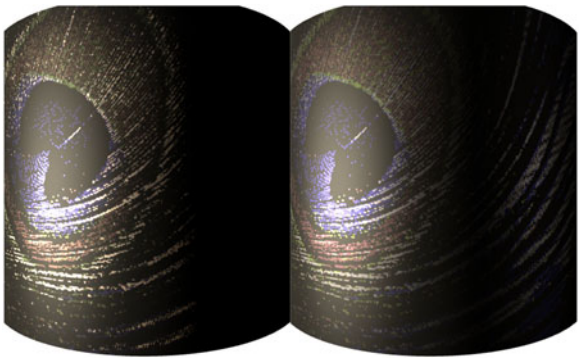

FIGURE 9. Same as in Figure 8 (left), but rendered without the secondary light (left) and using the standard model as well as the secondary light (right). The black paper underneath the mica particles has an additional reflectance that we model by a Phong highlight with low shininess and single scattering. The missing transmission of light is a limitation of our model.

Many features of the photographed sample are captured well by our model. Small discrepancies are likely due to partial overlap of the inks in some pixels.

DISCUSSION

Our method is suitable for capturing and modeling structural color particles arranged as a rough surface. The rendered result has a reasonable resemblance with the appearance of its physical counterparts. While our data were captured for a specific material, we believe our method is also useful for other similar materials. Because we took an outset in the Torrance–Sparrow model and did not modify the microfacet normal distribution function D, it is plausible that our model would also work well with other D-functions. We leave such an investigation for future work.

For a small angle of incidence, the goniometer we used did not allow measurement with the detector on the same side of the surface normal as the light source. We believe this leads to the bright subhighlights in the upper left parts of the spheres of Figure 5 rendered using measurements. Considering the trend in the other measurements with larger angle of incidence, where we were able to have the detector on the same side as the light source, we find our model plausible despite the fact that it does not exhibit a subhighlight of this kind. Denser measurements with a different goniometer could confirm this assumption.

Although our empirical parameters are not directly linked to physical parameters, we find them meaningful and editable. We found the spectral values of ρ and c to be within a certain range for all the three reflective inks that we measured. We believe that other spectra can be scaled and used to model other materials exhibiting different colors at normal and grazing angles of observation/incidence.

Because we measured primaries used for additive color printing, our method has a specific application in soft proofing for this type of printing.

Specific conditions, such as choice of paper, resolution, and halftoning algorithms affect the quality of the printed output. Our method can include these different aspects while also enabling interactive inspection to provide an impression of the appearance dynamics for different points of view.

An interesting extension of our model would be to capture material anisotropy effects, which we have observed during the sample preparation based on use of different brushing directions.

CONCLUSION

We presented a practical empirical BRDF model for representing readily available goniochromatic materials. By measuring the bidirectional reflectance of reflective inks, we demonstrated a practical application of our BRDF in print production where it enables soft proofing (preview) of halftoned additive color prints. Our model can interactively render this type of goniochromatic material with different surface roughnesses under varying light-view configurations. We hope our model can serve as a useful addition to the shader toolbox of the graphics practitioner.

ACKNOWLEDGMENTS

This work was supported by the European Union's Horizon 2020 research and innovation program under the Marie Skłdowska-Curie under Grant 814158 "ApPEARS."

Scanning electron microscope images were obtained thanks to ARTEMI, the Swedish Research Infrastructure for Advanced Electron Microscopy.

REFERENCES

1. G. Pfaff and J. Weitzel, "Pearlescent pigments/flakes," in *Coloring of Plastics: Fundamentals*, 2nd ed. Hoboken, NJ, USA: Wiley, 2004, ch. 15.
2. A. Pranovich, S. Valyukh, S. Gooran, J. R. Frisvad, and D. Nyström, "Dot off dot screen printing with RGBW reflective inks," *J. Imag. Sci. Technol.*, vol. 67, 2023, Art. no. 030404.
3. X. D. He, K. E. Torrance, F. X. Sillion, and D. P. Greenberg, "A comprehensive physical model for light reflection," *ACM SIGGRAPH Comput. Graphics*, vol. 25, no. 4, pp. 175–186, 1991.

4. J. S. Gondek, G. W. Meyer, and J. G. Newman, "Wavelength dependent reflectance functions," in *Proc. 21st Annu. Conf. Comput. Graphics Interactive Techn.*, 1994, pp. 213–220.
5. J. Stam, "Diffraction shaders," in *Proc. 26th Annu. Conf. Comput. Graphics Interactive Techn.*, 1999, pp. 101–110.
6. S. Ershov, K. Kolchin, and K. Myszkowski, "Rendering pearlescent appearance based on paint-composition modelling," *Comput. Graphics Forum*, vol. 20, no. 3, pp. 227–238, 2001.
7. A. Musbach, G. W. Meyer, F. Reitich, and S. H. Oh, "Full wave modelling of light propagation and reflection," *Comput. Graphics Forum*, vol. 32, no. 6, pp. 24–37, 2013.
8. I. Guillén, J. Marco, D. Gutierrez, W. Jakob, and A. Jarabo, "A general framework for pearlescent materials," *ACM Trans. Graphics*, vol. 39, no. 6, pp. 253:1–253:15, 2020.
9. K. E. Torrance and E. M. Sparrow, "Theory for off-specular reflection from roughened surfaces," *J. Opt. Soc. Amer.*, vol. 57, pp. 1105–1114, Sep. 1967.
10. J. F. Blinn, "Models of light reflections for computer synthesized pictures," in *Proc. 4th Annu. Conf. Comput. Graphics Interactive Techn.*, 1977, pp. 192–198.
11. T. S. Trowbridge and K. P. Reitz, "Average irregularity representation of a rough surface for ray reflection," *J. Opt. Soc. Amer.*, vol. 65, no. 5, pp. 531–536, 1975.
12. B. Walter, S. R. Marschner, H. Li, and K. E. Torrance, "Microfacet models for refraction through rough surfaces," in *Proc. 18th Eurograph. Conf. Rendering Techn.*, 2007, pp. 195–206.
13. F. Xie, J. Bieron, P. Peers, and P. Hanrahan, "Experimental analysis of multiple scattering BRDF models," in *Proc. SIGGRAPH Asia Tech. Commun.*, 2021, pp. 1–4.
14. D. S. Dhillon, J. Teyssier, M. Single, I. Gaponenko, M. C. Milinkovitch, and M. Zwicker, "Interactive diffraction from biological nanostructures," *Comput. Graphics Forum*, vol. 33, no. 8, pp. 177–188, 2014.
15. A. Toisoul and A. Ghosh, "Practical acquisition and rendering of diffraction effects in surface reflectance," *ACM Trans. Graphics*, vol. 36, no. 5, pp. 1–16, 2017.
16. V. Falster, A. Jarabo, and J. R. Frisvad, "Computing the bidirectional scattering of a microstructure using scalar diffraction theory and path tracing," *Comput. Graphics Forum*, vol. 39, no. 7, pp. 231–242, 2020.
17. L. Belcour and P. Barla, "A practical extension to microfacet theory for the modeling of varying iridescence," *ACM Trans. Graphics*, vol. 36, no. 4, pp. 1–14, 2017.
18. R. H. Muller and M. L. Sand, "Optimum angle of incidence for observing thin-film interference colors," *Appl. Opt.*, vol. 26, no. 24, pp. 5211–5220, 1987.
19. A. Pranovich et al., "Angular dependent reflectance spectroscopy of RGBW pigments," *Adv. Print. Media Technol.*, vol. XLVIII, pp. 19–24, 2023.
20. A. Trujillo-Vazquez, F. Abedini, A. Pranovich, C. Parraman, and S. Klein, "Printing with tonalli: Reproducing featherwork from precolonial Mexico using structural colorants," *Colorants*, vol. 2, no. 4, pp. 632–653, 2023.
21. S. Klein, C. Parraman, and L. Voges, "How to print a rainbow," *Proc. Printing Fabr.*, vol. 4, pp. 52–55, 2019. [Online]. Available: https://uwe-repository.worktribe.com/output/3257036/how-to-print-a-rainbow
22. G. J. Ward, "Measuring and modeling anisotropic reflection," *Comput. Graphics*, vol. 26, no. 2, pp. 265–272, 1992.
23. T. Tongbuasirilai, J. Unger, and M. Kurt, "Efficient BRDF sampling using projected deviation vector parameterization," in *Proc. Int. Conf. Comput. Vis. Workshops*, 2017, pp. 153–158.
24. R. L. Cook and K. E. Torrance, "A reflectance model for computer graphics," *Comput. Graphics*, vol. 15, no. 3, pp. 307–316, 1981.
25. K. Madsen, H. B. Nielsen, and O. Tingleff, "Methods for non-linear least squares problems," in *Lecture Notes*, 2nd ed., Technical Univ. Denmark, Denmark, 2004.
26. C. Schlick, "An inexpensive BRDF model for physically-based rendering," *Comput. Graphics Forum*, vol. 13, no. 3, pp. 233–246, 1994.
27. B. T. Phong, "Illumination for computer generated pictures," *Commun. ACM*, vol. 18, no. 6, pp. 311–317, 1975.
28. P. Hanrahan and W. Krueger, "Reflection from layered surfaces due to subsurface scattering," in *Proc. 20th Annu. Conf. Comput. Graphics Interactive Techn.*, 1993, pp. 165–174.

ALINA PRANOVICH is with Linköping University, 581 83, Norrköping, Sweden. She is the corresponding author of this article. Contact her at alina.pranovich@liu.se.

JEPPE REVALL FRISVAD is an associate professor at Technical University of Denmark, 2800, Kongens Lyngby, Denmark. His research is primarily on modeling and rendering of material appearance. Contact him at jerf@dtu.dk.

SERGIY VALYUKH is with Linköping University, 581 83, Linköping, Sweden. Contact him at sergiy.valyukh@liu.se.

SASAN GOORAN is with Linköping University, 581 83, Norrköping, Sweden. Contact him at sasan.gooran@liu.se.

DANIEL NYSTRÖM is with Linköping University, 581 83, Norrköping, Sweden. Contact him at daniel.nystrom@liu.se.